Grafting Activated Graphene Oxide Nanosheets onto Ultrafiltration Membranes Using Polydopamine to Enhance Antifouling Properties

Xiaoyi Chen^a, Erda Deng^a, Dongwon Park^a, Blaine A. Pfeifer^a, Ning Dai^b, and Haiqing Lin^a*

^a Department of Chemical and Biological Engineering, University at Buffalo, The State University of New York, Buffalo, NY 14260, USA

^b Department of Civil, Structural and Environmental Engineering, University at Buffalo, The State University of New York, Buffalo, NY 14260, USA

* Corresponding author. Tel: +1-716-645-1856, Email: haigingl@buffalo.edu (H. Lin)

ABSTRACT

Graphene oxide (GO) nanosheets are negatively charged and exhibit excellent antifouling

properties. However, their hydrophilicity makes it challenging for their grafting onto membrane

surfaces to improve antifouling properties for long-term underwater operation. Herein we

demonstrate a versatile approach to covalently graft GO onto ultrafiltration (UF) membrane

surfaces in aqueous solutions at ≈ 22 °C. The membrane surface is first primed using dopamine

and then reacted with activated GO (aGO) containing amine-reactive esters. The aGO grafting

improves the membrane surface hydrophilicity without decreasing water permeance. When the

membranes are challenged with 1.0 g/L sodium alginate in a constant-flux crossflow system, the

aGO grafting increases the critical flux by 20% and reduces the fouling rate by 63% compared

with the pristine membrane. The modified membranes demonstrate stability for 48-h operation and

interval cleanings using NaOH solutions.

KEYWORDS: Activated graphene oxide; ultrafiltration membranes; antifouling; polydopamine;

surface grafting

2

1. INTRODUCTION

Ultrafiltration (UF) membranes have been widely used for wastewater treatment and reuse due to their high energy-efficiency but are subject to fouling by contaminants in the feed water.¹⁻³ Fouling decreases water permeance and often increases transmembrane pressure to achieve desired productivity and thus energy consumption. Antifouling properties of the UF membranes can be improved by grafting with hydrophilic materials (such as zwitterionic materials^{4, 5} and poly(ethylene glycol)⁶) or non-stick materials (such as fluorochemicals⁷ and polysiloxanes⁸⁻¹⁰). There is an intensive effort in exploring new materials with superior antifouling properties for surface modification of state-of-the-art commercial membranes.

Graphene oxide (GO) nanosheets contain abundant oxygen-containing groups and can be highly hydrophilic. 11-14 Additionally, GO shows antimicrobial properties by inhibiting bacteria growth and even kills bacteria by disrupting the cell membranes. 15-17 Therefore, GO has been incorporated into membranes to increase antifouling and antimicrobial properties. 16-19 However, the hydrophilic GO must be covalently grafted onto the surface for long-term underwater operation. 15, 20 For example, GO nanosheets were first activated using 1-ethyl-3-(3-dimethylaminopropyl)carbodiimide (EDC) and *N*-hydroxysuccinimide (NHS) and then grafted onto polyamide-based membranes via ethylenediamine, which improved both antifouling and antimicrobial properties for forward osmosis applications. 20,21 Besides the carboxyl groups, epoxy and hydroxyl groups on the GO surface were also used for covalent grafting to the surface. 22, 23 However, these approaches require surfaces with specific functional groups or involve harsh

processing conditions such as repeated heating or UV irradiation, which restrict their practical applications. ^{22, 23}

Herein we demonstrate a versatile, substrate-independent approach to covalently graft GO onto polysulfone (PSf) UF membranes using dopamine without significantly decreasing water permeance, as shown in Figure 1. First, dopamine forms insoluble polydopamine (PDA) in an alkaline solution at ≈ 22 °C, which deposits on solid portions of the membrane surface without completely covering the pores.²⁴⁻²⁷ The PDA has been proposed to be polymers or colloids with H-bonds and π - π interactions.²⁸ The PDA coating had been demonstrated to be stable during the cleaning with hot water at 52 °C.²⁹ Second, the GO nanosheets were treated with H₂O₂ to reduce the size and then activated with EDC-NHS to convert the carboxyl groups to amine-reactive esters. Finally, the activated GO (aGO) nanosheets were grafted via the reaction of their esters groups with the amine groups on the PDA. The direct amide coupling between the carboxyl and amine groups typically occurs at 160°C or above due to the high activation barrier. 30, 31 The use of EDC-NHS as a coupling reagent enables the reaction at ~ 20 °C and improves yields to $\approx 85\%$.³² The EDC-NHS has also been successfully used to activate GO nanosheets before their grafting to the membranes with amine groups on the surface.^{20, 21}

The synergistic effect of the GO and PDA for membrane-related applications had been reported. For example, PDA was used to prepare multi-layer GO membranes for nanofiltration via surface-priming,³³ cross-linking,^{34, 35} intercalation,^{36, 37} and surface-protection.^{38, 39} PDA was also used to graft GO onto metal mesh surface for water/oil separation,⁴⁰ and directly graft GO (and with

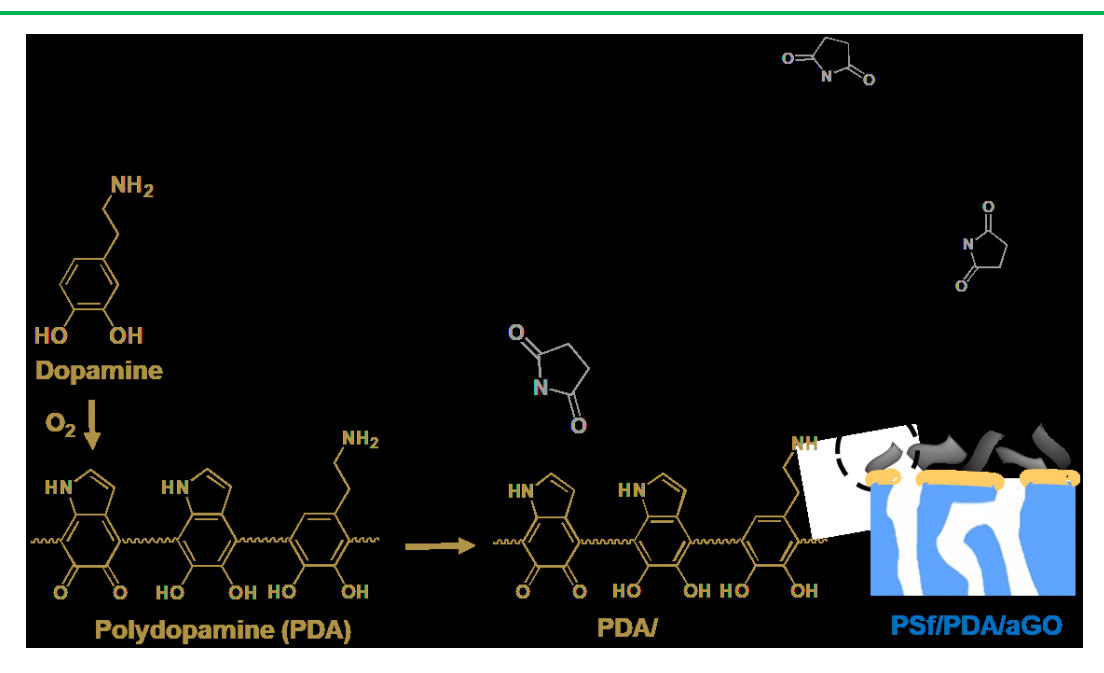


Figure 1. Schematic of the GO grafting onto the UF membrane (PSf/PDA/aGO), including three steps, PDA deposition on the surface, GO activation to form aGO, and the grafting of aGO by PDA. The R group refers to GO.

This work, for the first time, demonstrates the feasibility of grafting aGO with PDA to improve the efficiency of UF membranes for wastewater treatment and reuse. The effect of the aGO grafting on the membrane surface was thoroughly characterized, including hydrophilicity, roughness, pore coverage, and antimicrobial activity. The antifouling properties of the aGO-grafted membranes were determined using a constant-flux crossflow system with sodium alginate as a model foulant. The grafted aGO nanosheets demonstrate stability in \approx 48-h operation and resistance to cleaning using NaOH solutions. The surface modification occurs in aqueous solutions at \approx 22 °C and can be adapted to improve the performance of the state-of-the-art commercial membrane modules.²⁸,

42

2. RESULTS AND DISCUSSION

2.1 GO grafting and characterization

Figures 2a and 2b compare the GO nanosheets before and after the H₂O₂ treatment. The H₂O₂ is an oxidative agent and can remove the oxygenated carbon atoms, generating nanopores and eventually decreasing the GO nanosheet size.^{13, 43} In this work, all the GO used for the membrane preparation was treated for 5h (denoted as GO-5h) unless otherwise noted. The size reduction mitigates the aggregation of the GO nanosheets in the coating solutions and thus is expected to facilitate their grafting onto the surface. Increasing the H₂O₂ treatment time reduces the GO sheet size (as shown by the SEM images in Figure S1) and has a negligible effect on Zeta-potential (cf. Table S1) and defect structures (as shown by the Raman spectra in Figure S2).

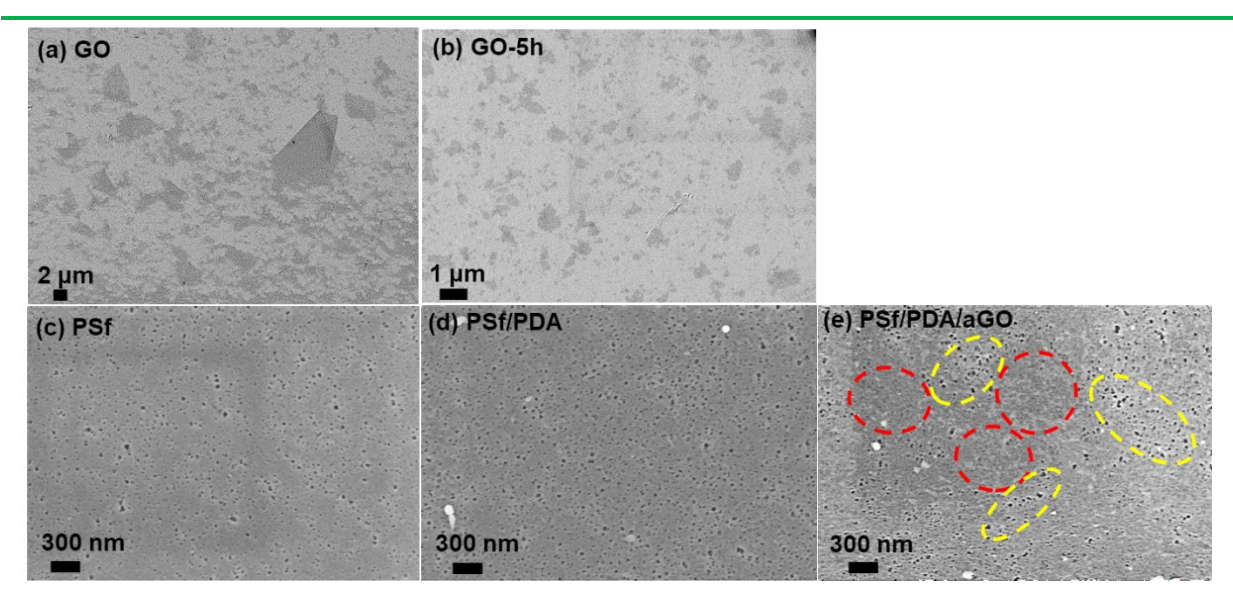


Figure 2. Characterization of the GO nanosheets and the modified membranes. SEM images of (a) GO and (b) GO-5h nanosheets on Si wafer. SEM images of the membrane surface for (c) PSf, (d) PSf/PDA, and (e) PSf/PDA/aGO. In (e), the yellow and red circles show the uncovered pores and covered pores on the membrane surface, respectively.

The thickness of the PDA layer on top of the PSf dense film on the Si wafers was determined to be 10 ± 2 nm, comparable to the values reported in the literature. The PDA/aGO layer shows almost the same thickness as the PDA layer, presumably because the GO sheets can only be covalently bonded by the carboxyl groups on their edges. As both dense films and membranes are made of PSf, the thickness of the coating layers is assumed to be the same for both substrates. However, since the PDA is not soluble in any solvent, the molecular weight and its impact on the aGO grafting efficiency cannot be determined.

Figures 2c-e confirm the GO grafting onto the membrane surface by SEM. The PSf/PDA displays a porous surface similar to the pristine PSf, indicating that the thin PDA coating does not completely cover the surface pores. The PDA coating has been reported to slightly decrease the surface pore size (or molecular weight cutoff).^{4, 44} After the aGO modification, the surface was partially covered by the aGO sheets (as marked by the red circles), while other pores remain open (marked by the yellow circles). The images of the Atomic Force Microscope (AFM) (cf. Figure S3) show that both the PDA/GO modification has a negligible effect on the roughness of the membrane surface. As the aGO nanosheet can be as thin as a few nanometers, direct observation or quantification of the aGO on the membrane surface remains challenging, and the successful grafting of the aGO is often implied by the changes to the surface properties.^{43, 46-48} Additionally, the PDA/aGO coating layer is too thin to observe in the cross-sectional SEM images, similar to the prior studies.^{4, 8, 42, 44}

2.2 Improved antifouling properties by aGO grafting

Figure 3a presents the effect of the membrane modification on the surface hydrophilicity, as indicated by the water contact angle. The PSf/PDA shows an average water contact angle of $58^{\circ} \pm 3^{\circ}$, the same as the PSf ($59^{\circ} \pm 2^{\circ}$), which is consistent with the literature.^{4, 49} By contrast, the PSf/PDA/aGO exhibits a water contact angle of $30^{\circ} \pm 3^{\circ}$, indicating a significantly enhanced hydrophilicity by the aGO grafting.

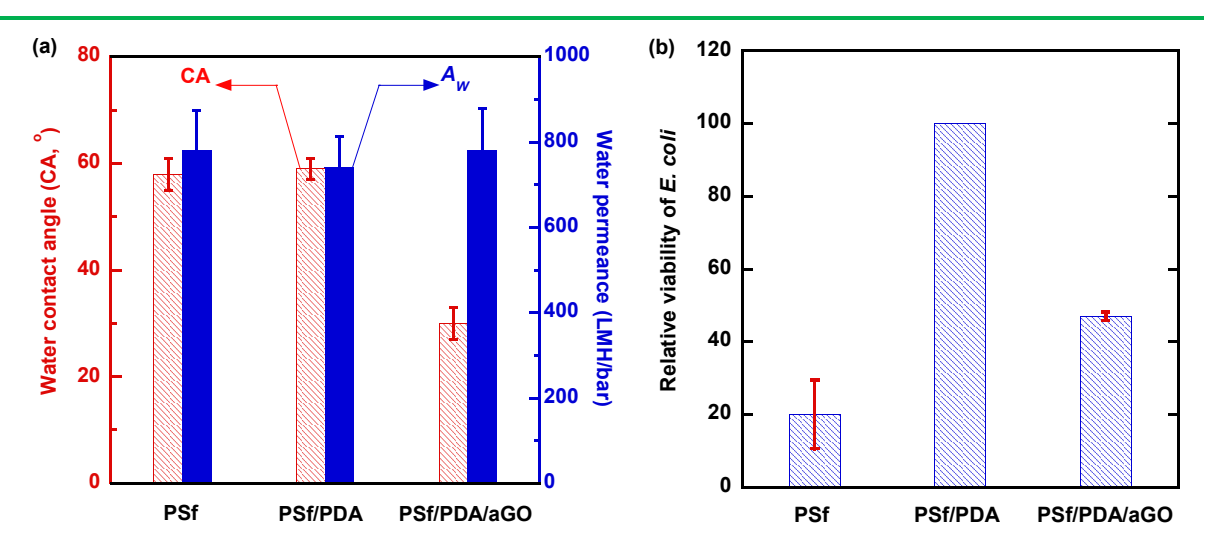


Figure 3. Effect of surface modification on (a) the water contact angle (CA) and water permeance for PSf UF membrane, and (b) the relative viability of *E. coli* to that for the PSf/PDA after contacting the surfaces for 3 h. The error bars represent one standard deviation from three repeated tests. In (a), the arrows point to the corresponding y-axis. In (b), PSf/PDA was chosen as the standard, and thus, no error bar is reported.

Figure 3a also shows that the effect of the surface modification on pure water permeance (A_w , L m⁻² h⁻¹ bar⁻¹, or LMH/bar), determined using a constant-flux crossflow system.⁴ The A_w can be calculated using equation 1:

$$A_w = \frac{Q_W}{A_m \Delta p} = \frac{J_W}{TMP} \tag{1}$$

where A_m is the active membrane area (m²), Δp is the transmembrane pressure (TMP, bar), and

Qw (L h⁻¹) and Jw (LMH) are the steady-state water flow rate and flux through the membrane, respectively. The coating of PDA or PDA/aGO has a negligible effect on the Aw, which can be ascribed to the thin coating layer (≈ 10 nm). The coating layer does not fully cover the pores, and the increased hydrophilicity caused by the aGO grafting also mitigates any adverse effect of the pore coverage on the water permeance.

Figure 3b illustrates the effect of surface modification on the antimicrobial properties, as indicated by the relative viability of *E. coli* with the PSf/PDA as the standard. For example, the relative viability for PSf equals the viability of PSf divided by the viability of PSf/PDA. The PDA coating increases the adhesion and thus the viability of *E. coli* on the membrane because it has a weak electrostatic repulsion with *E. coli*, ^{15, 50} while the aGO grafting reduces the viability of the *E. coli* by 53% compared with PSf/PDA, consistent with the hydrophilic and bactericidal properties of the GO. ^{15, 21, 51} However, PSf/PDA/aGO still shows higher viability of *E. coli* than PSf as the aGO nanosheets do not completely cover the PDA surface.

The antifouling properties of the membranes were evaluated using a flux-stepping method in the constant flux crossflow system with 1.0 g/L sodium alginate solution. Sodium alginate is a natural polysaccharide and a vital element for biofilm formation, and therefore, it has been widely used as a model foulant for investigating the membrane fouling during water purification.^{4, 52} As the system has two permeation cells in series,⁷ a pristine membrane sample was always used to directly compare with a modified sample to ensure the same testing conditions (including the flow rate, temperature, foulant content, etc.). It is very difficult to compare various surface modification

strategies for their efficiency to improve the antifouling properties because of the different testing conditions (such as membranes, foulants, flow conditions, etc.). On the other hand, the side-by-side comparison between the state-of-the-art commercial membrane and its modified version yields valuable information on the effect of surface modification and its potential for practical applications.

Figure 4 presents an example result for the PSf and PSf/PDA/aGO membranes, where J_W for both membranes was gradually increased from 15 LMH to 135 LMH at 15 LMH/step and 10 min for each step. Before the fouling test, the aGO modified membrane exhibits pure-water permeance of 830 LMH/bar, slightly higher than the PSf (730 LMH/bar), because of the improved surface hydrophilicity. At the J_W below 90 LMH, the TMP of both membranes remains constant, suggesting negligible fouling. After the J_W reaches 105 LMH, the TMP increases more rapidly for PSf than PSf/PDA/aGO, indicating the improved antifouling properties by aGO grafting caused by the improved surface hydrophilicity. Additionally, considering the negative charge of the alginate, the grafting of negatively charged aGO (cf. Table S1) can increase the electrostatic repulsion of the alginate, hindering its deposition onto the membrane surface. 53, 54

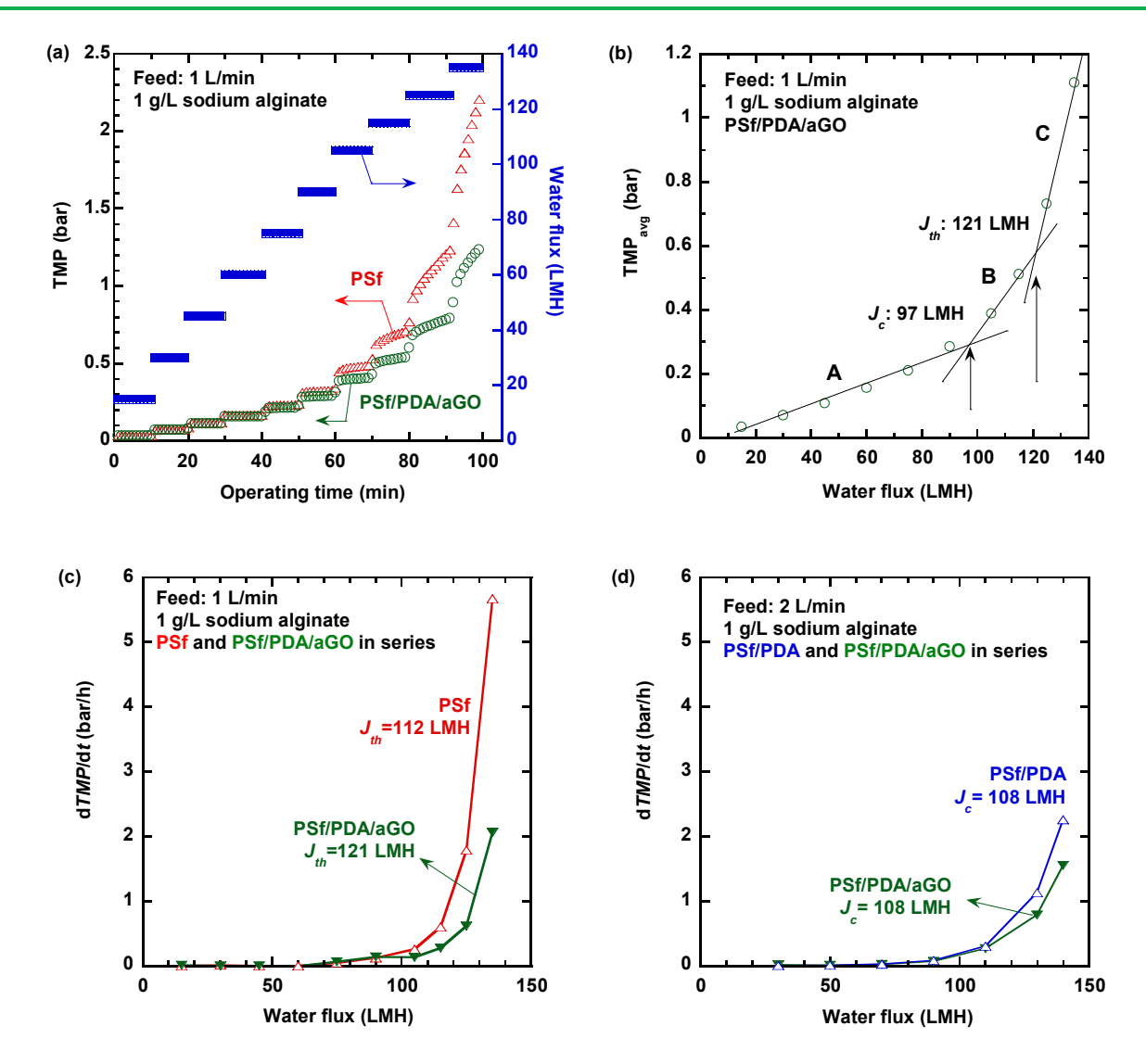


Figure 4. Improved antifouling properties of aGO-grafted PSf membranes in constant flux filtration tests with 1.0 g/L sodium alginate solution. (a) TMP and water flux (Jw) as a function of operating time (the arrows point to the corresponding y-axis). (b) TMP_{avg} and (c) dTMP/dt as a function of Jw in PSf and PSf/PDA/aGO at a feed flow rate of 1 L/min. (d) Comparison of the fouling rate in PSf/PDA and PSf/PDA/aGO at a feed flow rate of 2 L/min.

The fouling resistance of the membranes can be characterized by the critical flux (J_c , below which the TMP remains constant with time) and the threshold flux (J_{th} , above which the TMP increases significantly with time).^{4, 44, 55} Industrial membranes are often operated below their J_{th}

values to avoid rapid fouling. Figure 4b illustrates the determination of J_c and J_{th} . Based on the flux-stepping tests (cf. Figure 4a), the average TMP (TMP_{avg}) at each flux is calculated and plotted with J_W . The data can be separated into three regions (A, B, and C) according to the slopes. The intersection between the first (A) and second (B) linear region is defined as J_c , while the intersection of the second (B) and third (C) region is J_{th} . PSf/PDA/aGO membrane exhibits the J_{th} value of 121 LMH, higher than the PSf (112 LMH), confirming the improved antifouling property by aGO grafting.

Figure 4c compares the dTMP/dt values at each flux for PSf and PSf/PDA/aGO. At J_W below 90 LMH (below J_c), both membranes show negligible fouling. At J_W above 105 LMH, dTMP/dt values increase significantly, while PSf/PDA/aGO exhibits lower dTMP/dt values than PSf. For example, the dTMP/dt reduces by 63% from 5.7 bar/h in PSf to 2.1 bar/h in PSf/PDA/aGO at J_W of 135 LMH. Figure S4 also confirms the improved antifouling properties by the aGO grafting at a higher feed flow rate (1.5 L/min corresponding to a Reynolds number of 1350), instead of 1 L/min (a Reynolds number of 900). Increasing the Reynolds number also increases the J_{th} values for both membranes, consistent with the increased shear force caused by increasing the flow rate.

Figure 4d directly elucidates the improved antifouling behavior derived from aGO grafting by comparing PSf/PDA and PSf/PDA/aGO. The *TMP* and *Jw* values as a function of the operating time are presented in Figure S7a. At the *Jw* above 130 LMH, the aGO grafting reduces the fouling rate by 30% compared with the PSf/PDA. Additionally, Figures 4c and 4d show that increasing the feed flow rate from 1 L/h to 2 L/h (and thus the Reynolds number from 900 to 1800) can

significantly decrease the dTMP/dt values. As a result, the J_w exceeds the limit of the mass flow controller before the J_{th} can be determined in Figure 4d.

The effect of the H_2O_2 treating time for the GO on the membrane performance was also investigated. As the treatment time increases from 2 h to 9 h, the values of J_{th} and dTMP/dt remain almost constant (cf. Figure S5 and Table S2), though all the aGO-grafted samples show lower dTMP/dt values than the pristine PSf. Figure S6 shows that grafting with 1 g/L or 0.1 g/L aGO solution has a similar effect in improving the antifouling properties compared with the pristine PSf. However, optimizing the concentration of aGO in the grafting is beyond the scope of this study.

Figures S7b and S7c display the antifouling test for PSf/PDA and PSf/PDA/aGO when challenged by 5.0 g/L sodium alginate at a feed flow rate of 1.5 L/min. The increased sodium alginate concentration accelerates the fouling rate for both membranes. However, the PSf/PDA/aGO still shows 17% less fouling rate than PSf/PDA.

Figure 5 displays the SEM images of PSf and PSf/PDA/aGO surfaces after the 4-h fouling by sodium alginate. The aGO-grafted membranes show a smoother surface than the pristine one, suggesting the improved antifouling properties.^{17, 44, 56} Both fouled membranes exhibit rougher surfaces than the pristine ones (cf. Figure 2). Figures 5c and 5f also show that the deposition of the foulant on the surface covers the pores, decreasing the water permeance.

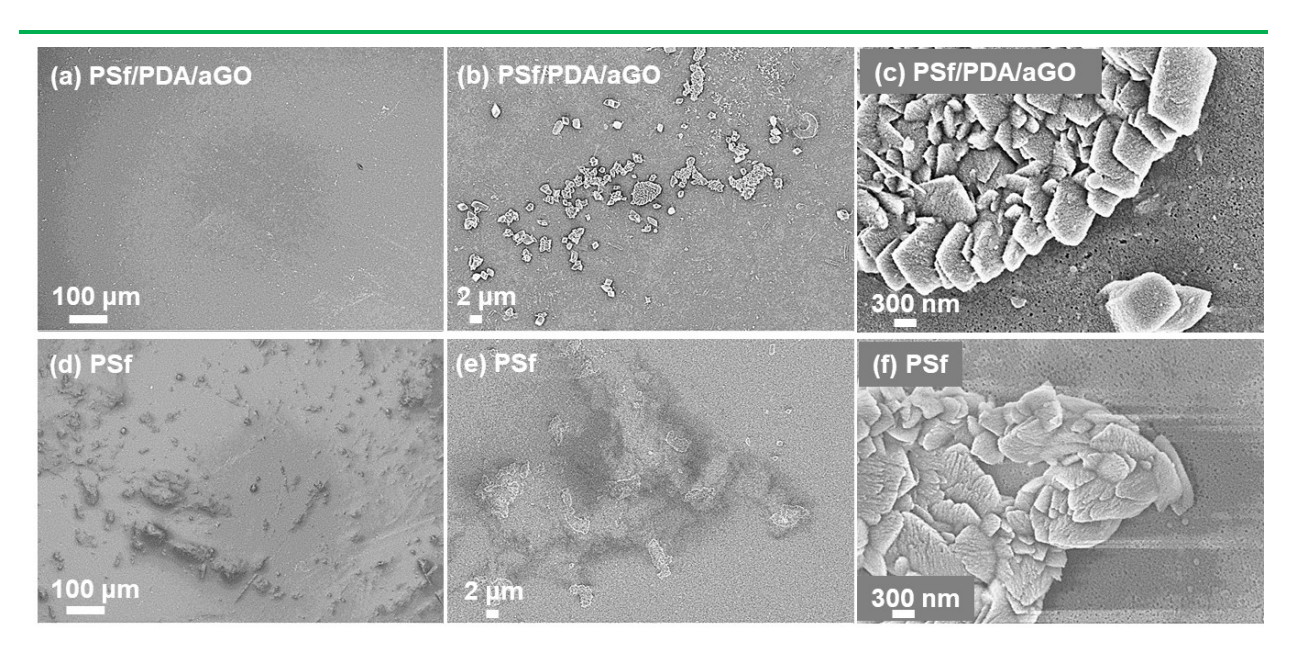


Figure 5. SEM images of the membrane surface fouled by sodium alginate. (a), (b), and (c): PSf/PDA/aGO at different magnifications; (d), (e), and (f): PSf at different magnifications. The 4-h fouling was conducted with 1.0 g/L sodium alginate at a feed flow rate of 1 L/min and J_W of 130 LMH.

2.3 Continuous operation and cleaning of the modified membranes

Figure 6a demonstrates the stability of the surface modification via 48-h continuous crossflow operation with 1.0 g/L sodium alginate. The PSf/PDA/aGO exhibits a lower A_W value (770 LMH/bar) than the PSf (830 LMH/bar). The J_W was set at 85 LMH, below the J_{th} values and above the J_c values, and thus both membranes showed fouling behavior. At the beginning of the filtration, the TMP of the membranes were comparable, despite the lower A_W value in PSf/PDA/aGO. After the 10-h operation, the aGO-grafted membrane exhibits lower TMP values than the pristine PSf, indicating the improved antifouling properties by the aGO grafting.

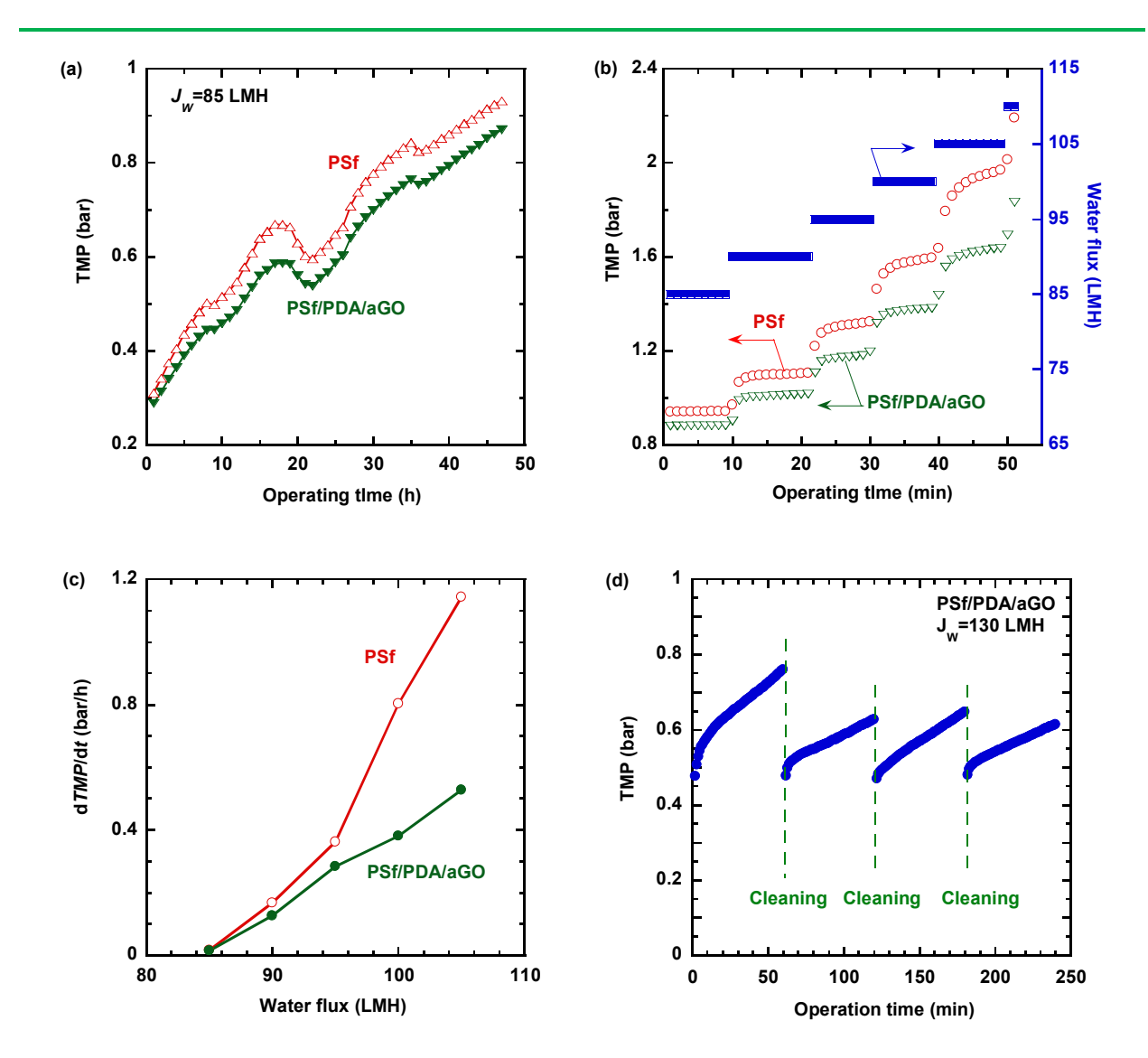


Figure 6. Long-term stability of the aGO-grafted PSf membranes tested with 1.0 g/L sodium alginate. TMP as a function of operating time (a) in the first 48 h at J_W of 85 LMH and (b) continuous flux-stepping tests at various J_W values for 50 min (the arrows point to the corresponding y-axis). (c) dTMP/dt as a function of J_W in the flux-stepping test. (d) TMP evolution in PSf/PDA/aGO membrane during the multiple fouling-cleaning cycles at the feed flow rate of 1 L/min. For (a), the decrease of TMP at \approx 17 h is presumably caused by a fluctuation of the feed pressure.

Figure 6b displays the 50-min flux-stepping test results after the 48-h continuous test for both membranes. The TMP increases with increasing J_W values, and the increase is slower for

PSf/PDA/aGO than PSf. Figure 6c presents the dTMP/dt values as a function of Jw. At Jw above 95 LMH, the PSf exhibits accelerated fouling while the aGO-grafted membrane does not. At Jw of 105 LMH, PSF/PDA/aGO shows dTMP/dt of 0.53 bar/h, 54% lower than the PSf (1.1 bar/h). These tests demonstrate the stability of the membranes and PDA/aGO coating during the \sim 48-h test. Longer-term stability tests will be needed for the membranes to be considered, and the impact of the aGO and dopamine on the quality of clean water needs to be addressed for practical applications. However, it is beyond the scope of this study.

As the foulant accumulates on the surface, the membranes can be cleaned using chemical agents. Figure 6d displays the effect of cleaning on the performance recovery for PSf/PDA/aGO in a multi-cycle fouling-cleaning experiment. The membrane was challenged by 1.0 g/L sodium alginate at J_W of 130 LMH, above its J_{th} for accelerated fouling. After 60-min operation, the membrane was cleaned using an aqueous NaOH solution (pH of 11) in the crossflow system for 30 min. The fouling-cleaning process was repeated for 4 times (cf. Figure 6d) while the cleaning is not displayed for simplification. During the first fouling test, the TMP increases by 58% from 0.48 bar to 0.76 bar and then decreases to 0.48 bar after the cleaning, the same as the initial TMP value, indicating that the cleaning completely recovers the membrane performance. In the following fouling-cleaning cycles, the TMP remains within a range between 0.48 bar and 0.65 bar, confirming the stability of the aGO-grafted membranes, their resistance to chemical cleaning, and promise for industrial applications.

3. CONCLUSION

We demonstrate a facile approach to covalently graft hydrophilic GO onto the UF membrane surface using PDA. A thin PDA layer (≈ 10 nm) can be deposited on PSf membranes without fully covering the pores or significantly decreasing water permeance, while the amine groups react with the ester groups on the aGO to allow grafting of the aGO in a robust manner. The aGO grafting increases surface hydrophilicity and retains high water permeance in alginate fouling tests compared with PSf and PSf/PDA. In a constant-flux crossflow system, the aGO grafting can reduce the fouling rate by 63%. After the 48-h continuous test, the PSf/PDA/aGO exhibits 54% lower fouling rate than the pristine PSf, confirming the integrity and effectiveness of the aGO grafting over a long time. The fouled PSf/PDA/aGO membranes were cleaned using a NaOH solution, leading to nearly 100% recovery of water permeance. The surface modification of membranes with dopamine and aGO occurs in aqueous solutions at ≈ 22 °C, and thus, it may be used for the post-modification of commercial membrane modules for industrial uses.

4. EXPERIMENTAL SECTION

Materials. Natural graphite powder (325 mesh) was purchased from Qingdao Huatai Graphite Co. (Qingdao, China). H₂SO₄ (99%), H₂O₂ (30 wt.% in H₂O), KMnO₄ (\geq 99.0%), dopamine hydrochloride, Trizma base (\geq 99.9%), 2-(*N*-morpholino) ethanesulfonic acid (MES, \geq 99.0%), EDC (\geq 98%), NHS (\geq 98%), and sodium alginate were procured from Sigma-Aldrich Corporation (St. Louis, MO). HCl (2.0 M) and ethanol (95%) were supplied by VWR International

(Radnor, PA). PSf100 UF membrane (with molecular weight cutoff of 100 kDa) was purchased from Alfa Laval AB (Lund, Sweden). NaOH and sterile 0.9 % saline solution were obtained from Fisher Scientific International (Hampton, NH). Lysogeny Broth (LB) and LB agar were purchased from Thermo Fisher Scientific (Waltham, MA).

Preparation of GO and PSf/PDA/aGO membranes. GO was prepared from graphite using the modified Hummers' method. A3, First, graphite (3 g) was added to concentrated H₂SO₄ (70 mL) followed by the gradual addition of KMnO₄ (9 g) in an ice bath (below 20 °C). The solution was then moved to a 40 °C water bath and stirred for 30 min. Second, water (150 mL) was added to the solution, which was then heated at 90 °C for 15 min before more water (500 mL) was added. H₂O₂ was then gradually added to remove the residual KMnO₄ or manganese dioxide. Third, GO was obtained by filtration and then washed with HCl solution and deionized water before purification by centrifugation and dispersion in deionized (DI) water by ultrasonication. Finally, H₂O₂ (10 mL) was added to 2 g/L GO solution (100 mL), which was then heated at 100 °C for 5 h for GO oxidation to reduce the sheet size. The final GO product was obtained by dialysis and centrifugation. Although this approach of GO production involves aggressive chemicals, more environmentally friendly processes have also been developed. The formula from the production involves aggressive chemicals, more

The GO was grafted onto the PSf membrane surface in three steps. First, the membrane surface was exposed to a 2.0 g/L dopamine solution for 1 h using a rocking platform shaker (VWR International, Radnor, PA) with the tilt of level 6 and shaking speed of 30.^{4, 42} The membrane was then rinsed with and sonicated in deionized water to remove the unbonded PDA. Second, to

prepare aGO, 0.1 g/L GO was dispersed in 10 mM MES buffer by sonication, and then 2 mM EDC and 5 mM NHS were added before 15-min sonication to convert the carboxyl groups to amine-reactive esters. The pH of the solution was then adjusted to 8.0 using NaOH. Finally, the PDA coated membrane was exposed to the aGO solution for 3 h. The membrane was then rinsed using DI water and kept in water before uses.

Characterization. The GO nanosheets and membrane surface were imaged using a focused ion beam scanning electron microscope (FIB-SEM, Carl Zeiss Auriga CrossBeam, Carl Zeiss Germany). Surface hydrophilicity was characterized using a Ramé Hart contact angle goniometer (Model 190, Succasunna, NJ). Raman spectra of GO with various H₂O₂ treatment times were collected using Raman spectroscopy (Renishaw InVia, UK) with a 514 nm laser source. The charge of GO solution was characterized using a dynamic light scattering analyzer (Zetasizer Nano, Malvern, Worcestershire, UK). The surface morphology of PSf/PDA/aGO and pristine membranes was characterized using AFM (Bruker Dimension Icon with ScanAsyst, Bruker, Germany) in the tapping mode. The AFM probe is TESPA-V2 (Bruker, Germany) with a nominal spring constant of 42 N/m.

The thickness of the PDA layer on the membrane cannot be measured due to the interference from the uncovered surface pores. 4, 42, 61 Instead, thin dense PSf films (~ 100 nm) on silicon wafers were used as substrates for PDA coating. First, the wafers were cleaned using acetone and blowdried. Second, a 4 wt% PSf in cyclopentanone was spin-coated on the wafer using an MTC-100 spin coater (MicroNano Tools, Canada) at 40% relative humidity. The spin rate was set as 500

rpm for 3 s followed by 4000 rpm for 60 s. Finally, dopamine was deposited on the PSf following the same procedures for the membrane modification. Multi-wavelength ellipsometry (FS-1, Film Sense, NE) was used to determine the thickness of the PDA layer.⁴²

The antimicrobial activity of the PSf/PDA/aGO membranes was evaluated using a plate counting method. 15, 62 Escherichia coli (E. coli, BL21(DE3), New England BioLabs) was used as the model bacteria. First, the cells were cultivated in lysogeny broth (LB) (3 mL) overnight at 37 °C. Then the cultures were diluted in 30 mL of LB (1:100) and grown until the exponential phase was reached (OD₆₀₀ 0.6). The E. coli suspension was diluted to around 8×10^8 CFU mL⁻¹ before use (where CFU denotes colony-forming unit). Second, the membrane samples were cut into small coupons with an effective area of 3.9 cm² and placed in the holders for the surface to expose to the E. coli suspension (2 mL) for 1 h. The membrane samples were then rinsed by applying gentle flow drops of sterile 0.9% saline solution to both sides to remove the free bacteria that did not adhere to the membranes. The rinsing process for all the membrane samples was the same to ensure a valid comparison. Third, the membranes were placed in the saline solution (12 mL) and sonicated for 8 min at 40 HZ to detach the bacteria from the surface. Three aliquots of each resulting saline solution were mixed in LB broth to achieve 10², 10³, and 10⁴ dilution ratios, respectively. The diluted solution was then spread evenly on an LB agar for plate counting. After 15 min of drying in a sterile condition, the LB agar plates were placed in a 36 °C incubator overnight. The number of colonies on the plate reflects the viability of the bacteria cells on the membrane surface, which relates to its antimicrobial property.

Pure water permeance was determined using a custom-made constant-flux crossflow system.⁴

In the measurement, the Ow was set to constants using a mass flow controller on the permeate

while the *TMP* was monitored. The constant-flux crossflow system was also used to determine the

antifouling properties of the membranes with 1.0 g/L sodium alginate as a model foulant.⁴ The

feed pressure was held constant while the permeate pressure decreased to retain the targeted Ow.

The increase of TMP with time (dTMP/dt) reflects the fouling rate of the membrane.

■ ASSOCIATED CONTENT

Supporting Information

The Supporting Information is available free of charge on the ACS publications website. Details

on the GO characterization and the antifouling properties of the aGO-modified membranes, and

supplementary figures and tables (PDF).

■ AUTHOR INFORMATION

Corresponding Author

*E-mail: haiqingl@buffalo.edu (H. Lin)

ORCID

Haiqing Lin: 0000-0001-8042-154X

Author Contributions

The manuscript was prepared through the contributions of all authors. All authors have approved

the final version of the manuscript.

21

Notes

The authors declare no conflict of interest.

■ ACKNOWLEDGMENT

We gratefully acknowledge the financial support from the U.S. National Science Foundation (NSF

Award No. 1635026) and the U.S. Department of Interior (DOI Award No. R17AC00147).

■ REFERENCES

- 1. Miller, D. J.; Dreyer, D. R.; Bielawski, C. W.; Paul, D. R.; Freeman, B. D., Surface Modification of Water Purification Membranes, *Angew. Chem. Int. Ed.* **2017**, *56* (17), 4662-4711.
- 2. Zhang, R.; Liu, Y.; He, M.; Su, Y.; Zhao, X.; Elimelech, M.; Jiang, Z., Antifouling Membranes for Sustainable Water Purification: Strategies And Mechanisms, *Chem. Soc. Rev.* **2016**, *45* (21), 5888-5924.
- 3. Shahkaramipour, N.; Tran, T. N.; Ramanan, S.; Lin, H., Membranes with Surface-enhanced Antifouling Properties for Water Purification, *Membranes* **2017**, *7* (1), 13.
- 4. Shahkaramipour, N.; Jafari, A.; Tran, T.; Stafford, C. M.; Cheng, C.; Lin, H., Maximizing the Grafting of Zwitterions onto the Surface of Ultrafiltration Membranes to Improve Antifouling Properties, *J. Membr. Sci.* **2020**, *601*, 117909.
- 5. Kirschner, A.; Chang, C.; Kasemset, S.; Emrick, T.; Freeman, B. D., Fouling-resistant Ultrafiltration Membranes Prepared via Co-deposition of Dopamine/Zwitterion Composite Coatings, *J. Membr. Sci.* **2017**, *541* (1), 300-311.
- 6. McCloskey, B. D.; Park, H. B.; Ju, H.; Rowe, B. W.; Miller, D. J.; Freeman, B. D., A Bioinspired Fouling-resistant Surface Modification for Water Purification Membranes, *J. Membr. Sci.* **2012**, *413*, 82-90.
- 7. Tran, T.; Tu, Y.-C.; Hall-Laureano, S.; Lin, C.; Kawy, M.; Lin, H., "Nonstick" Membranes Prepared by Facile Surface Fluorination for Water Purification, *Ind. Eng. Chem. Res.* **2020**, *59* (12), 5307-5314.
- 8. Tran, T.; Chen, X.; Doshi, S.; Stafford, C. M.; Lin, H., Grafting Polysiloxane onto Ultrafiltration Membranes to Optimize Surface Energy and Mitigate Fouling, *Soft Matter* **2020**, *16*, 5044-5053.
- 9. Zhao, X.; Su, Y.; Li, Y.; Zhang, R.; Zhao, J.; Jiang, Z., Engineering Amphiphilic Membrane

- Surfaces based on PEO and PDMS Segments for Improved Antifouling Performances, *J. Membr. Sci.* **2014**, *450*, 111-123.
- 10. Pi, J.; Yang, J.; Xu, Z., One-Pot Mussel-Inspiration and Silication: A Platform for Constructing Oil-Repellent Surfaces toward Crude Oil/Water Separation, *J. Membr. Sci.* **2020**, *601*, 117915.
- 11. Ang, E. Y. M.; Toh, W.; Yeo, J.; Lin, R.; Liu, Z.; Geethalakshmi, K. R.; Ng, T. Y., A Review on Low Dimensional Carbon Desalination and Gas Separation Membrane Designs, *J. Membr. Sci.* **2020**, *598*, 117785.
- 12. Yang, T.; Lin, H.; Loh, K. P.; Jia, B., Fundamental Transport Mechanisms and Advancements of Graphene Oxide Membranes for Molecular Separation, *Chem. Mater.* **2019**, *31* (6), 1829-1846.
- 13. Liu, G.; Jin, W.; Xu, N., Graphene-based Membranes, Chem. Soc. Rev. 2015, 44, 5016-5030.
- 14. Du, Y.; Zhang, X.; Yang, J.; Lv, Y.; Zhang, C.; Xu, Z., Ultra-Thin Graphene Oxide Films Via Contra-Diffusion Method: Fast Fabrication for Ion Rejection, *J. Membr. Sci.* **2020**, *595*, 117586.
- 15. Cheng, W.; Lu, X.; Kaneda, M.; Zhang, W.; Bernstein, R.; Ma, J.; Elimelech, M., Graphene Oxide-functionalized Membranes: The Importance of Nanosheet Surface Exposure for Biofouling Resistance, *Environ. Sci. Technol.* **2020**, *54* (1), 517-526.
- 16. Chen, L.; Shi, G.; Shen, J.; Peng, B.; Zhang, B.; Wang, Y.; Bian, F.; Wang, J.; Li, D.; Qian, Z.; Xu, G.; Liu, G.; Zeng, J.; Zhang, L.; Yang, Y.; Zhou, G.; Wu, M.; Jin, W.; Li, J.; Fang, H., Ion Sieving in Graphene Oxide Membranes via Cationic Control of Interlayer Spacing, *Nature* **2017**, *550* (7676), 415-418.
- 17. Perreault, F.; De Faria, A. F.; Elimelech, M., Environmental Applications of Graphene-based Nanomaterials, *Chem. Soc. Rev.* **2015**, *44* (16), 5861-5896.
- 18. Chang, Y.; Shen, Y.; Kong, D.; Ning, J.; Xiao, Z.; Liang, J.; Zhi, L., Fabrication of the Reduced Preoxidized Graphene-based Nanofiltration Membranes with Tunable Porosity and Good Performance, *RSC Adv.* **2017**, *7* (5), 2544-2549.
- 19. Xue, J.; BinAhmed, S.; Wang, Z.; Karp, N. G.; Stottrup, B. L.; Romero-Vargas Castrillón, S., Bacterial Adhesion to Graphene Oxide (GO)-functionalized Interfaces Is Determined by Hydrophobicity and GO Sheet Spatial Orientation, *Environ. Sci. Technol. Lett.* **2017**, *5* (1), 14-19. 20. Perreault, F.; Jaramillo, H.; Xie, M.; Ude, M.; Nghiem, L. D.; Elimelech, M., Biofouling
- Mitigation in Forward Osmosis Using Graphene Oxide Functionalized Thin-film Composite Membranes, *Environ. Sci. Technol.* **2016**, *50* (11), 5840-5848.
- 21. Kaneda, M.; Lu, X.; Cheng, W.; Zhou, X.; Bernstein, R.; Zhang, W.; Kimura, K.; Elimelech, M., Photografting Graphene Oxide to Inert Membrane Materials to Impart Antibacterial Activity, *Environ. Sci. Technol. Lett.* **2019**, *6* (3), 141-147.
- 22. Wang, J.; Gao, X.; Wang, J.; Wei, Y.; Li, Z.; Gao, C., O-(carboxymethyl)-chitosan Nanofiltration Membrane Surface Functionalized with Graphene Oxide Nanosheets for Enhanced Desalting Properties, *ACS Appl. Mater. Interfaces* **2015**, *7* (7), 4381-4389.
- 23. Igbinigun, E.; Fennell, Y.; Malaisamy, R.; Jones, K. L.; Morris, V., Graphene Oxide Functionalized Polyethersulfone Membrane to Reduce Organic Fouling, *J. Membr. Sci.* **2016**, *514*, 518-526.

- 24. Ryu, J.; Messersmith, P. B.; Lee, H., Polydopamine Surface Chemistry: A Decade of Discovery, *ACS Appl. Mater. Interfaces* **2018**, *10* (9), 7523-7540.
- 25. Yang, H.; Waldman, R. Z.; Wu, M.; Hou, J.; Chen, L.; Darling, S. B.; Xu, Z., Dopamine: Just the Right Medicine for Membranes, *Adv. Funct. Mater.* **2018**, *28* (8), 1705327.
- 26. Lee, H.; Dellatore, S. M.; Miller, W. M.; Messersmith, P. B., Mussel-inspired Surface Chemistry for Multifunctional Coatings, *Science* **2007**, *318* (5849), 426-430.
- 27. Pi, J.; Yang, J.; Zhong, Q.; Wu, M.-B.; Yang, H.; Schwartzkopf, M.; Roth, S. V.; Müller-Buschbaum, P.; Xu, Z., Dual-Layer Nanofilms Via Mussel-Inspiration and Silication for Non-Iridescent Structural Color Spectrum in Flexible Displays, *ACS Appl. Nano Mater.* **2020,** *2* (7), 4556-4566.
- 28. Dreyer, D. R.; Miller, D. J.; Freeman, B. D.; Paul, D. R.; Bielawski, C. W., Perspectives on Poly(dopamine), *Chem. Sci.* **2013**, *4* (10), 3796-3802.
- 29. Miller, D. J.; Huang, X.; Li, H.; Kasemset, S.; Lee, A.; Agnihotri, D.; Hayes, T.; Paul, D. R.; Freeman, B. D., Fouling-resistant Membranes for the Treatment of Flowback Water from Hydraulic Shale Fracturing: A Pilot Study, *J. Membr. Sci.* **2013**, *437*, 265-275.
- 30. Al-Zoubi, R. M.; Marion, O.; Hall, D. G., Direct and Waste-free Amidations and Cycloadditions by organocatalytic Activation of carboxylic Acids at Room Temperature, *Angew. Chem. Int. Ed.* **2008**, *47* (15), 2876-2879.
- 31. Lundberg, H.; Tinnis, F.; Selander, N.; Adolfsson, H., Catalytic Amide Formation from Non-activated Carboxylic Acids and Amines, *Chem. Soc. Rev.* **2014**, *43* (8), 2714-2742.
- 32. Valeur, E.; Bradley, M., Amide Bond Formation: Beyond the Myth of Coupling Reagents, *Chem. Soc. Rev.* **2009**, *38* (2), 606-631.
- 33. Wang, C.; Li, Z.; Chen, J.; Yin, Y.; Wu, H., Structurally Stable Graphene Oxide-based Nanofiltration Membranes with Bioadhesive Polydopamine Coating, *Appl. Surf. Sci.* **2018**, *427*, 1092-1098.
- 34. Cui, W.; Li, M.; Liu, J.; Wang, B.; Zhang, C.; Jiang, L.; Cheng, Q., A Strong Integrated Strength and Toughness Artificial Nacre Based on Dopamine Cross-linked Graphene Oxide, *ACS Nano* **2014**, *8* (9), 9511-9517.
- 35. Zhang, Y.; Chen, S.; An, J.; Fu, H.; Wu, X.; Pang, C.; Gao, H., Construction of An Antibacterial Membrane based on Dopamine and Polyethylenimine Cross-linked Graphene Oxide, *ACS Biomater. Sci. Eng.* **2019**, *5* (6), 2732-2739.
- 36. Xu, Y.; Wu, M.; Yu, S.; Zhao, Y.; Gao, C.; Shen, J., Ultrathin and Stable Graphene Oxide Film via Intercalation Polymerization of Polydopamine for Preparation of Digital Inkjet Printing Dye, *J. Membr. Sci.* **2019**, *586*, 15-22.
- 37. Liu, L.; Xie, X.; Zambare, R. S.; Selvaraj, A. P. J.; Sowrirajalu, B.; Song, X.; Tang, C.; Gao, C., Functionalized Graphene Oxide Modified Polyethersulfone Membranes for Low-pressure Anionic Dye/Salt Fractionation, *Polymers* **2018**, *10* (7), 795.
- 38. Liu, N.; Zhang, M.; Zhang, W.; Cao, Y.; Chen, Y.; Lin, X.; Xu, L.; Li, C.; Feng, L.; Wei, Y., Ultralight Free-standing Reduced Graphene Oxide Membranes for Oil-in-water Emulsion

- Separation, J. Mater. Chem. A 2015, 3 (40), 20113-20117.
- 39. Li, Y.; Shi, S.; Gao, H.; Zhao, Z.; Su, C.; Wen, H., Improvement of the Antifouling Performance and Stability of An Anion Exchange Membrane by Surface Modification with Graphene Oxide (GO) and Polydopamine (PDA), *J. Membr. Sci.* **2018**, *566*, 44-53.
- 40. Yin, Y.; Li, H.; Zhu, L.; Guo, T.; Li, X.; Xing, W.; Xue, Q., A Durable Mesh Decorated with Polydopamine/Graphene Oxide for Highly Efficient Oil/Water Mixture Separation, *Appl. Surf. Sci.* **2019**, *479*, 351-359.
- 41. Hao, X.; Chen, S.; Zhu, H.; Wang, L.; Zhang, Y.; Yin, Y., The Synergy of Graphene Oxide and Polydopamine Assisted Immobilization of Lysozyme to Improve Antibacterial Properties, *Chemistryselect* **2017**, *2* (6), 2174-2182.
- 42. Shahkaramipour, N.; Ramanan, S. N.; Fister, D.; Park, E.; Venna, S. R.; Sun, H.; Cheng, C.; Lin, H., Facile Grafting of Zwitterions onto the Membrane Surface to Enhance Antifouling Properties for Wastewater Reuse, *Ind. Eng. Chem. Res.* **2017**, *56* (32), 9202-9212.
- 43. Chen, X.; Feng, Z.; Gohil, J.; Stafford, C. M.; Dai, N.; Huang, L.; Lin, H., Reduced Holey Graphene Oxide Membranes for Desalination with Improved Water Permeance, *ACS Appl. Mater. Interfaces* **2020**, *12* (1), 1387-1394.
- 44. Kasemset, S.; Wang, L.; He, Z.; Miller, D. J.; Kirschner, A.; Freeman, B. D.; Sharma, M. M., Influence of Polydopamine Deposition Conditions on Hydraulic Permeability, Sieving Coefficients, Pore Size and Pore Size Distribution for A Polysulfone Ultrafiltration Membrane, *J. Membr. Sci.* **2017**, *522*, 100-115.
- 45. Schneider, A.; Hemmerle, J.; Allais, M.; Didierjean, J.; Michel, M.; d'Ischia, M.; Ball, V., Boric Acid as An Efficient Agent for the Control of Polydopamine Self-assembly and Surface Properties, *ACS Appl. Mater. Interfaces* **2018**, *10* (9), 7574-7580.
- 46. Huang, L.; Huang, S.; Venna, S. R.; Lin, H., Rightsizing Nanochannels in Reduced Graphene Oxide Membranes by Solvating for Dye Desalination, *Environ. Sci. Technol.* **2018**, *52* (21), 12649-12655.
- 47. Anand, A.; Unnikrishnan, B.; Mao, J.; Lin, H.; Huang, C., Graphene-based Nanofiltration Membranes for Improving Salt Rejection, Water Flux and Antifouling-A Review, *Desalination* **2018**, *429*, 119-133.
- 48. Yang, Q.; Su, Y.; Chi, C.; Cherian, C. T.; Huang, K.; Kravets, V. G.; Wang, F.; Zhang, J.; Pratt, A.; Grigorenko, A. N.; Guinea, F.; Geim, A. K.; Nair, R. R., Ultrathin Graphene-based Membrane with Precise Molecular Sieving and Ultrafast Solvent Permeation, *Nat. Mater.* **2017**, *16* (12), 1198-1201.
- 49. Kasemset, S.; Lee, A.; Miller, D. J.; Freeman, B. D.; Sharma, M. M., Effect of Polydopamine Deposition Conditions on Fouling Resistance, Physical Properties, and Permeation Properties of Reverse Osmosis Membranes in Oil/Water Separation, *J. Membr. Sci.* **2013**, *425*, 208-216.
- 50. Cui, J.; Ju, Y.; Liang, K.; Ejima, H.; Lörcher, S.; Gause, K. T.; Richardson, J. J.; Caruso, F., Nanoscale Engineering of Low-fouling Surfaces through Polydopamine Immobilisation of Zwitterionic Peptides, *Soft Matter* **2014**, *10* (15), 2656-2663.

- 51. Zhang, W.; Cheng, W.; Ziemann, E.; Be'er, A.; Lu, X.; Elimelech, M.; Bernstein, R., Functionalization of Ultrafiltration Membrane with Polyampholyte Hydrogel and Graphene Oxide to Achieve Dual Antifouling and Antibacterial Properties, *J. Membr. Sci.* **2018**, *565*, 293-302.
- 52. Weinman, S. T.; Husson, S. M., Influence of Chemical Coating Combined with Nanopatterning on Alginate Fouling During Nanofiltration, *J. Membr. Sci.* **2016**, *513*, 146-154.
- 53. Kumar, M.; Sreedhar, N.; Jaoude, M. A.; Arafat, H. A., High-Flux, Antifouling Hydrophilized Ultrafiltration Membranes with Tunable Charge Density Combining Sulfonated Poly(ether sulfone) and Aminated Graphene Oxide Nanohybrid, *ACS Appl. Mater. Interfaces* **2020**, *12* (1), 1617-1627.
- 54. Hadidi, M.; Buckley, J. J.; Zydney, A. L., Effect of Electrostatic Interactions on the Ultrafiltration Behavior of Charged Bacterial Capsular Polysaccharides, *Biotechnol. Prog.* **2016**, *32* (6), 1531-1538.
- 55. Kirschner, A. Y.; Cheng, Y.-H.; Paul, D. R.; Field, R. W.; Freeman, B. D., Fouling Mechanisms in Constant Flux Crossflow Ultrafiltration, *J. Membr. Sci.* **2019**, *574*, 65-75.
- 56. Han, J.; Haider, M. R.; Liu, M.; Wang, H.; Jiang, W.; Ding, Y.; Hou, Y.; Cheng, H.; Xia, X.; Wang, A., Borate Inorganic Cross-linked Durable Graphene Oxide Membrane Preparation and Membrane Fouling Control, *Environ. Sci. Technol.* **2019**, *53* (3), 1501-1508.
- 57. Lowe, S. E.; Zhong, Y., Challenges of Industrial-Scale Graphene Oxide Production. In *Graphene Oxide: Fundamentals and Applications*, Dimiev, A. M.; Eigler, S., Eds. Wiley: 2016; pp 410-431.
- 58. Lowe, S. E.; Shi, G.; Zhang, Y.; Qin, J.; Wang, S.; Uijtendaal, A.; Sun, J.; Jiang, L.; Jiang, S.; Qi, D., Scalable Production of Graphene Oxide Using a 3D-printed Packed-bed Electrochemical Reactor with a Boron-doped Diamond Electrode, *ACS Appl. Nano Mater.* **2019**, *2* (2), 867-878.
- 59. Yang, E.; Karahan, H. E.; Goh, K.; Chuah, C. Y.; Wang, R.; Bae, T.-H., Scalable Fabrication of Graphene-based Laminate Membranes for Liquid and Gas Separations by Crosslinking-induced Gelation and Doctor-blade Casting, *Carbon* **2019**, *155*, 129-137.
- 60. Rathour, R. K. S.; Bhattacharya, J., A Green Approach for Single-pot Synthesis of Graphene Oxide and Its Composite with Mn₃O₄, *Appl. Surf. Sci.* **2018**, *437*, 41-50.
- 61. Ramanan, S. N.; Shahkaramipour, N.; Tran, T.; Zhu, L.; Venna, S. R.; Lim, C.-K.; Singh, A.; Prasad, P. N.; Lin, H., Self-cleaning Membranes for Water Purification by Co-deposition of Photomobile 4, 4'-azodianiline and Bio-adhesive Polydopamine, *J. Membr. Sci.* **2018**, *554*, 164-174.
- 62. Perreault, F.; Tousley, M. E.; Elimelech, M., Thin-film Composite Polyamide Membranes Functionalized with Biocidal Graphene Oxide Nanosheets, *Environ. Sci. Technol. Lett.* **2014,** *I* (1), 71-76.

Table of Contents Graphic

